On the Role of Intermediate States for Artificial Spin Ice Inspired Computation

Hanu Arava[1], Ignacio T. Tapia[2], Timothy Cote[1,3], Justin S. Woods[1], Frank Barrows[4], John Fullerton[1], and Paula Mellado[2]

[1]Materials Science Division, Argonne National Laboratory, Lemont, IL 60439, USA

[2]School of Engineering and Sciences, Adolfo Ibáñez University, Santiago 7910000, Chile

[3]Department of Materials Science and Engineering, Northwestern University, Evanston, IL 60208, USA

[4]Center for Nonlinear Studies, Los Alamos National Laboratory, Los Alamos, NM 87545, USA

I. Scanning Electron Microscope (SEM)

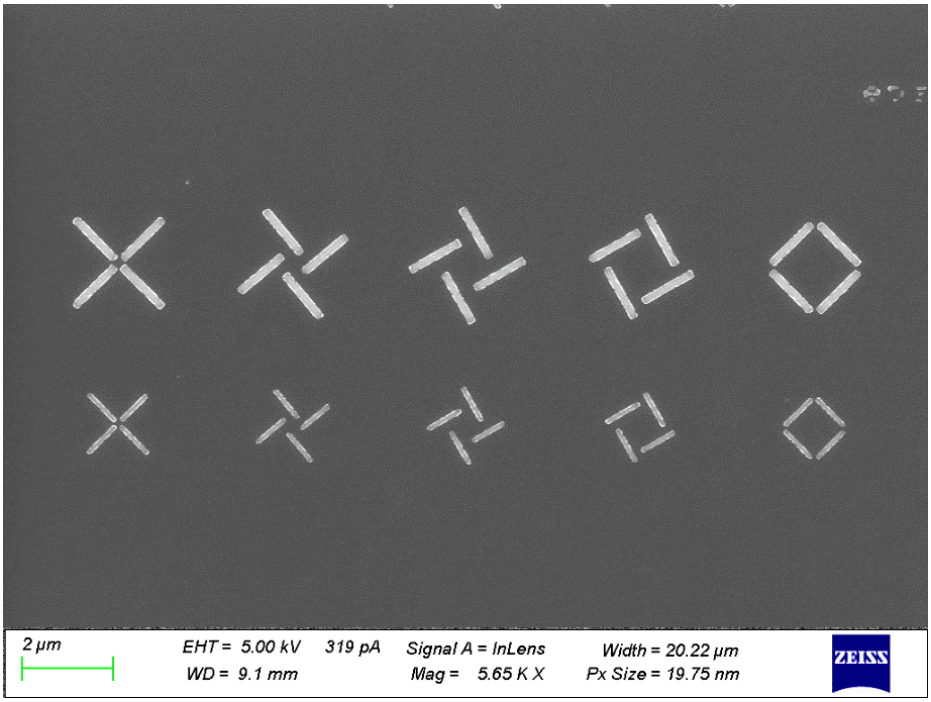

Fig. 1: Scanning Electron Microscope (SEM) images of the toy model for $\epsilon = 0.15$ and $\epsilon = 0.3$ respectively.

II. Magnetic Force Microscope (MFM) Data

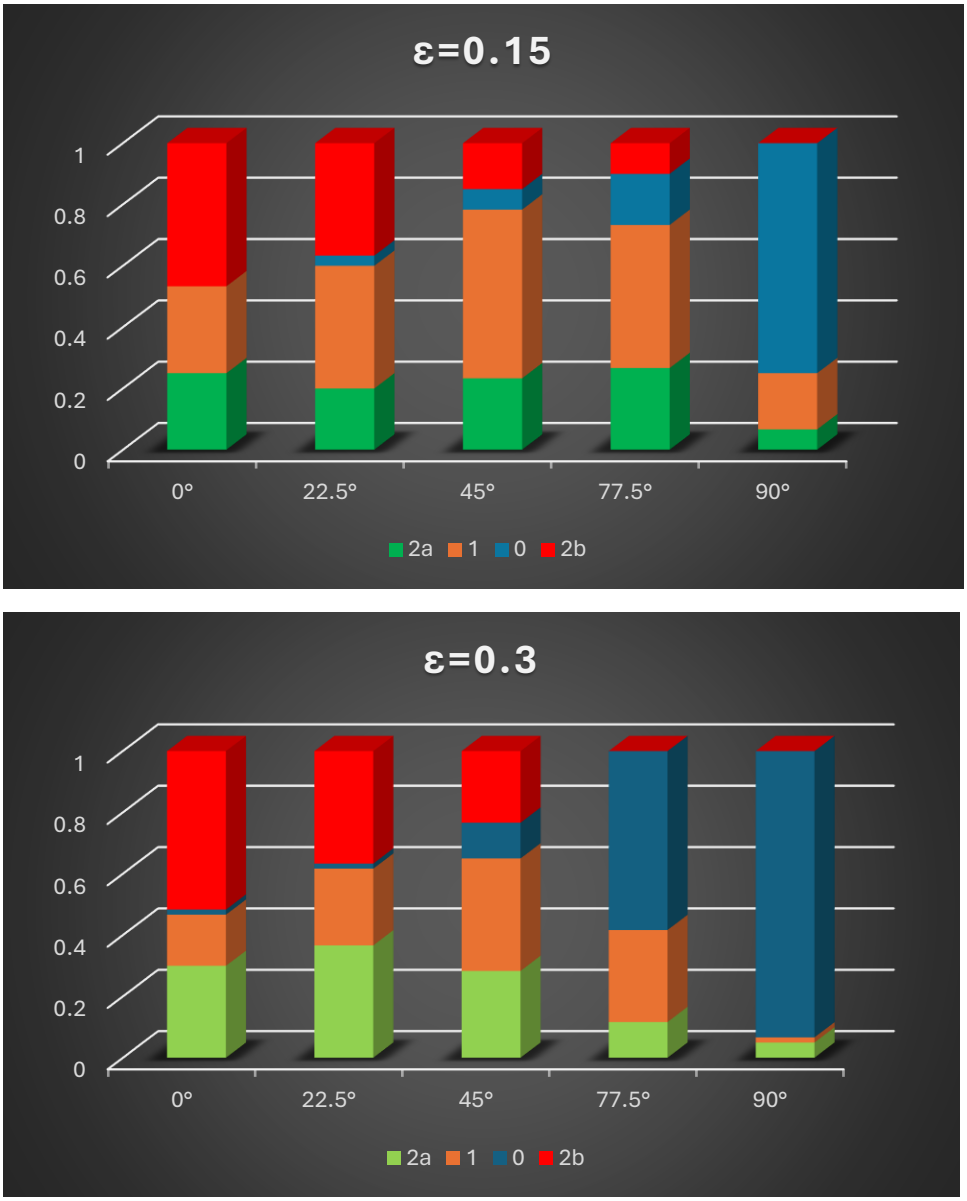

Fig. 2: Normalized fraction of the experimentally observed states in 60 structures for each of the $\epsilon = 0.15$ and $\epsilon = 0.3$. The data was collected from MFM scans, with all the structures initialized in state 2*a* and underwent a field-induced non ergodic energy relaxation as described in the main text.

III. Description of the system

Consider a cluster consisting of four nanomagnets arranged with their centers lying in the middle point of the sides of a square plaquette of side a, at positions $\vec{r}_n = \frac{a}{2}(\cos\theta_n, \sin\theta_n)$, with $\theta_n = 2(n-1)\frac{\pi}{4}$, $n = 1, \ldots, 4$. We define the length of the magnets $l = a(1-\epsilon)$, in terms of $\epsilon \in (0,1)$ which is a constant scaling factor. The magnets are oriented in direction $\hat{\mu}_n = (\cos(\theta_n + \phi), \sin(\theta_n + \phi))$, where $\phi \in [0, \pi/2]$ defines the rotation of a magnetic island in the plane of the plaquette with respect to its local z axis fixed in its center as shown in Fig.4a. Each magnet n has an uniform magnetization density, and its magnetic moment $\vec{m}_n$ is constrained to point in the direction of its long axis $\vec{m}_n = \pm m_0 \hat{\mu}_n$, being effectively an Ising-like degree of freedom. The magnitude of the magnetic moment is $m_0 = ql$ with $q = A_T M_s$, where M_s is the magnetization of saturation of permalloy and A_T is the cross section of the nanomagnet.

As shown in Fig.5, there are $2^4 = 16$ possible states for the magnetic configuration of the cluster, defined by the orientation of the magnetic moment at each island.

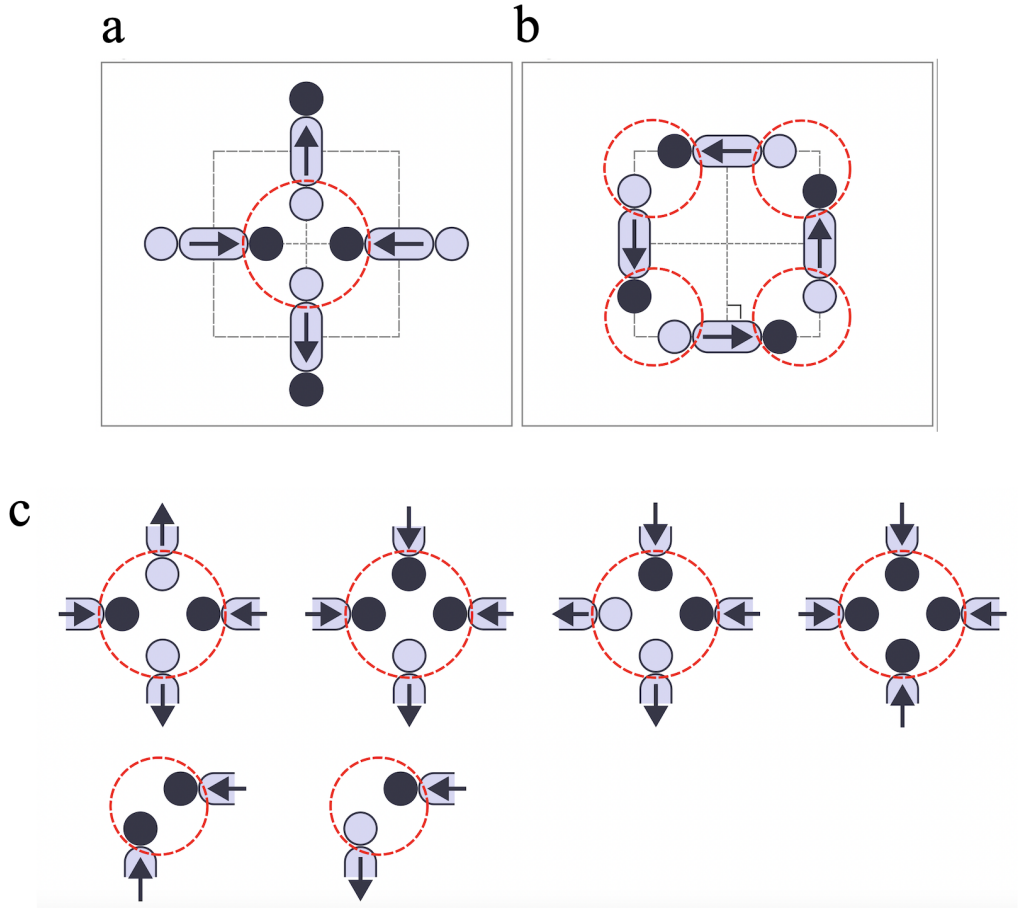

FIG. 3: Dumbbell (purple and black dots) and dipolar (arrows) models for magnetic nanoisland. Enclosed by a dotted red circle are nodes giving rise to multipolar structures. In (a) a Vertex plaquette is shown in its ground state magnetic configuration 2*b*. In (b) a Loop plaquette is shown in its ground state 0.

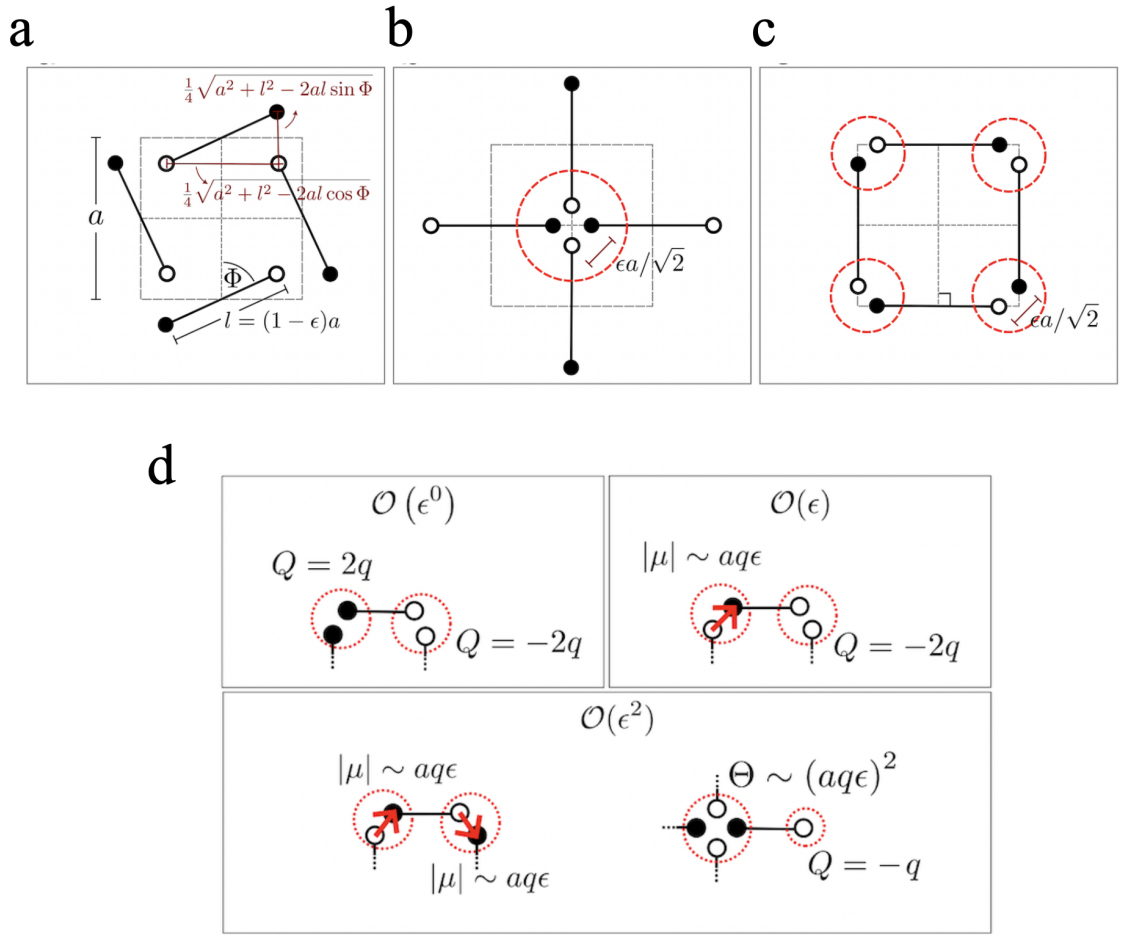

FIG. 4: a) Geometric description of the system in terms of the length of a magnet, $l=(1-\epsilon)a$, where a is the length of the side of the square lattice where the magnetic plaquette is inscribed. $\phi\in[0,\pi/2]$ dubbed the rotation angle defines the arrangement of the magnetic island. b)A vertex structure in state 2b depicts two -q and two +q changes at the central node. Two q charges of opposite sign form a tiny magnetic dipole whose magnitutude is proportional to ϵ. c) A loop plaquette in the state 0, two q charges form dipoles at the corners of the square. d) Schematics of multipolar moments such as the monopole Q, dipoles μ and quadrupoles Θ.

When a is much larger than l, the magnets can be modeled as point dipoles. Therefore, the magnetic energy of the plaquette E_{mag} can be approximated by a dipolar energy given by the interaction among such dipoles

$$E_{\rm dip}=-\frac{\mu_0}{4\pi}\sum_{n<k}\frac{(\vec{m}_n\cdot\hat{r}_{nk})(\vec{m}_k\cdot\hat{r}_{nk})-\vec{m}_n\cdot\vec{m}_k}{r_{nk}^3} \tag{1}$$

where $\vec{r}_{nk}=\vec{r}_n-\vec{r}_k$ is the center-to-center distance between dipoles.

However, when the distance between the center of two magnets is smaller than half their length, the dipolar model is not a good approximation for their magnetic coupling [1]. In this case instead of considering each island as a point dipole Fig.3, the magnetostatic energy of the system, E_{mag} is better approximated by the Coulomb energy due to interactions between charges at the tips of the magnets: each nanomagnet is modelled as a dumbbell with two magnetic charges $\pm q$ lying at its ends as shown in Fig.3. The positions of the charges $\vec{r}_n^{\pm}$ can be written in terms of

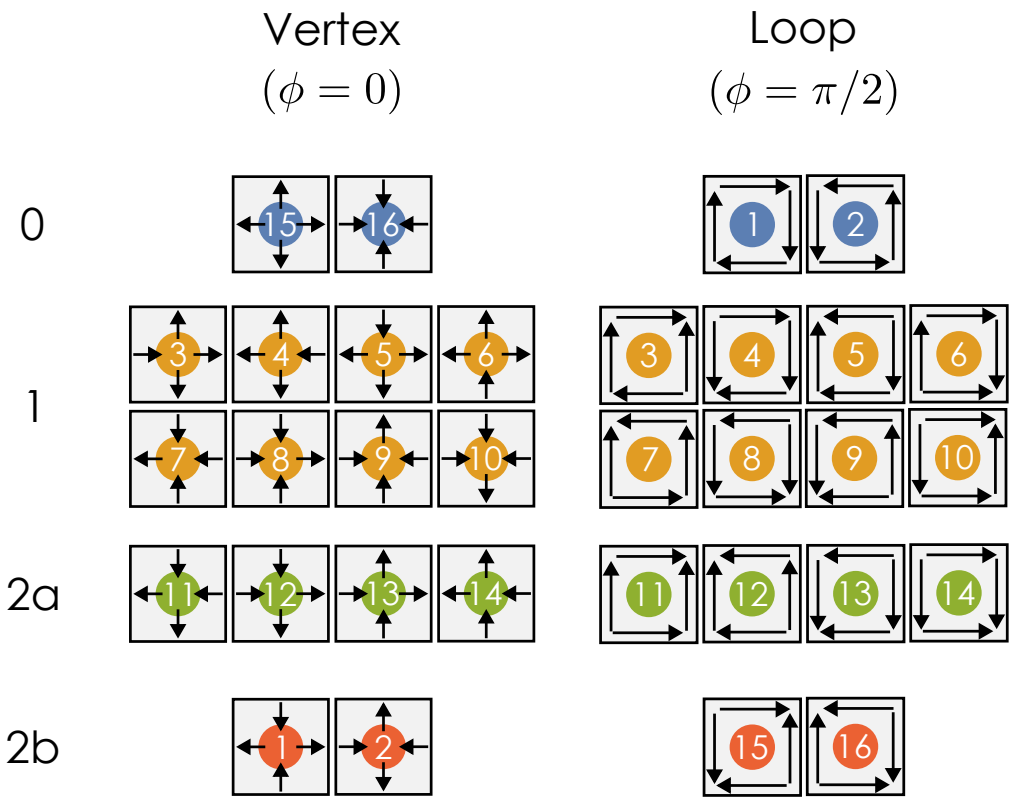

FIG. 5: Four inequivalent families of magnetic configurations for the Loop and Vertex plquettes. Plaquettes in the same family have the same E_{dip} and same E_c. The color convention and nomenclature will be used in every figure that involves these configurations.

magnetic moment of the magnetic islands, $\vec{m}_n$, as

$$\vec{r}_n^{\pm} = \vec{r}_n \pm \frac{a}{2}(1-\epsilon)\,, \quad \hat{m}_n = \vec{r}_n \pm \frac{1}{2q}\vec{m}_n\,, \tag{2}$$

where $\vec{r}_n^{+}$ and $\vec{r}_n^{-}$ are the positions of the positive and negative charges of island n, respectively.

In the dumbbell model the energy for a system of charges can be written as a Coulomb interaction given by

$$E_{\rm c} = \frac{\mu_0 q^2}{4\pi}\sum_{n<k}\left(\frac{1}{|\vec{r}_n^{+} - \vec{r}_k^{+}|} + \frac{1}{|\vec{r}_n^{-} - \vec{r}_k^{-}|} - \frac{1}{|\vec{r}_n^{-} - \vec{r}_k^{+}|} - \frac{1}{|\vec{r}_n^{+} - \vec{r}_k^{-}|}\right) \tag{3}$$

IV. Loop and Vertex plaquettes

Due to the square point symmetry of square plaquettes, for every possible value of ϕ there are four inequivalent families of configurations as shown in Figs.5 and 6. We start our analysis with the Vertex and Loop geometries that arise for $\phi = 0$ and $\phi = \pi/2$, respectively. The Vertex and Loop geometries are such that in the limit $\epsilon \to 0$ the tips of

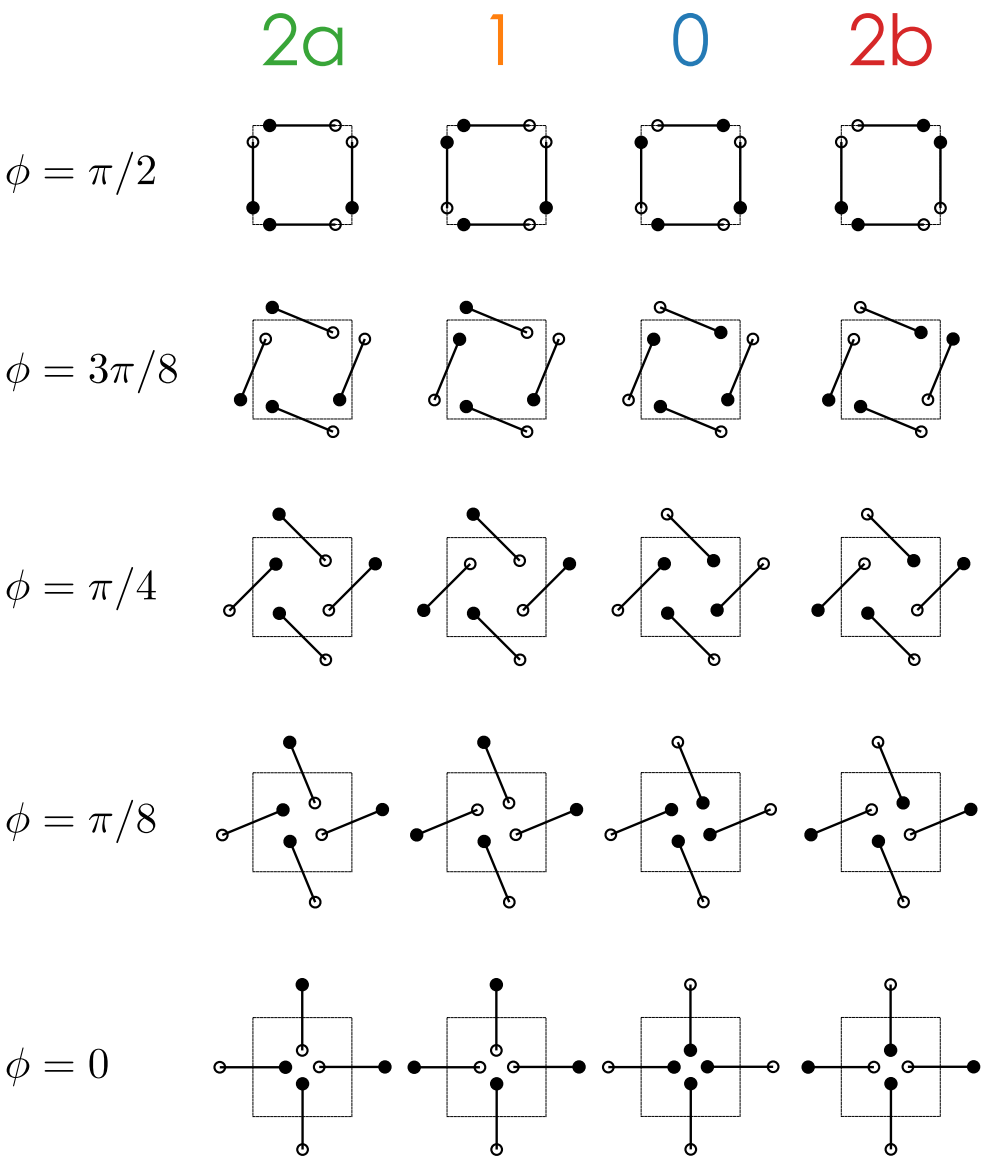

FIG. 6: Inequivalent families of configurations for different geometries of the system as a function of ϕ.

adjacent islands touch. The specific configurations in each of these arrangements can be grouped in four inequivalent families, with magnetic configurations in each family sharing a common energy. We named these configurations 0, 1, 2a and 2b, 5.

In the limit $\epsilon \to 1$, the coulomb interactions between charges at the tips of islands coincide with the dipolar interactions, as can be seen in figure 9. The dipolar energy depends on ϵ, but only through a quadratic scaling with the length of the island. For small values of ϵ the dipolar interactions miss the detail of the close range interactions, as the energy between nearest neighbour charges becomes dominant. The dumbbell model provides a description for the regime in which the islands are close, lifting the non-trivial degeneracies that appear in the dipolar description,

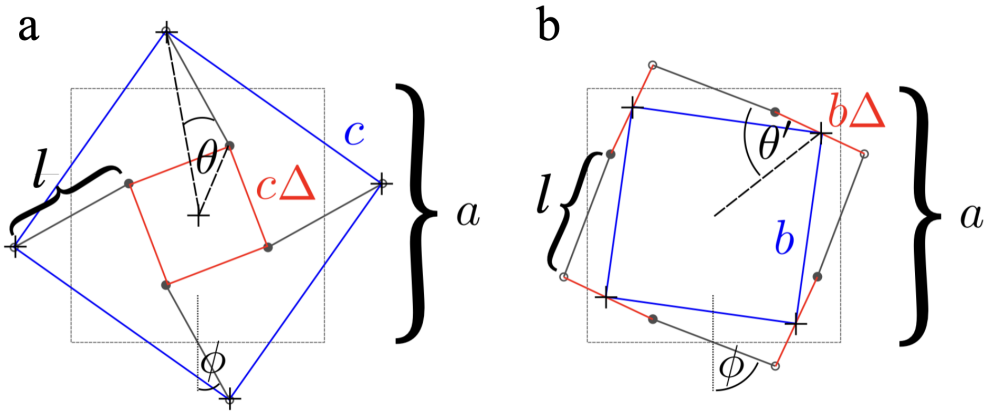

FIG. 7: Schematics of the geometric quantities defined to compute the multipolar expansion in the case of clusters close to the Vertex (a) and Loop (b) plaquettes.

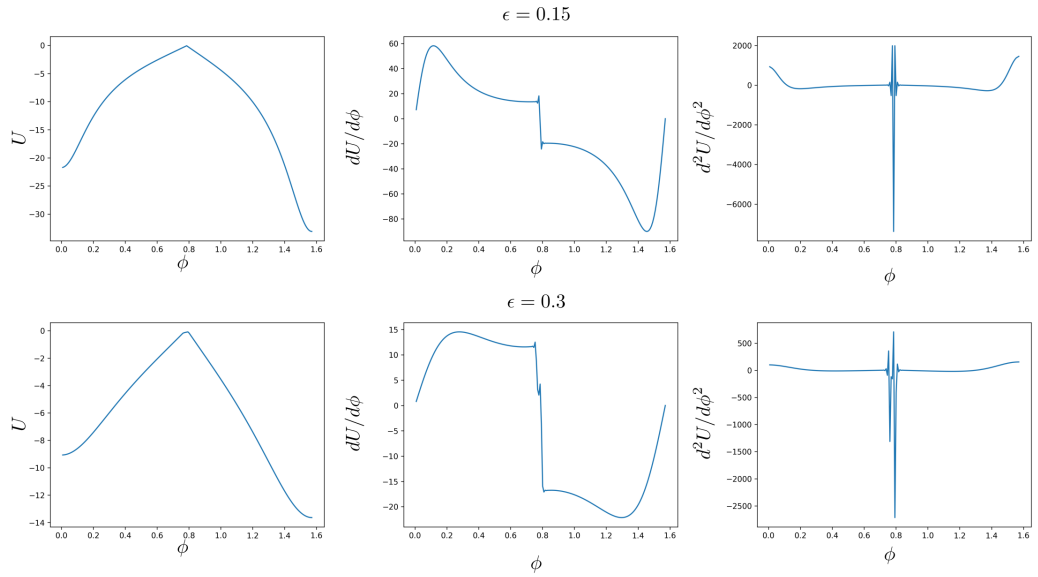

FIG. 8: For the case of $\epsilon = 0.15$ (top) and $\epsilon = 0.3$ (bottom), the left panel shows the ground state coulomb energy of clusters as a function of the rotation angle ϕ. Its first and second derivatives are depicted in the middle and right panels respectively.

as discussed below.

A. Multipolar Expansion

For Vertex and Loop geometries, in the limit $\epsilon \to 0$, the tips of adjacent islands share the same position. We can use this fact to expand the Coulomb energy around $\epsilon = 0$ to understand the relaxation pathways of square plaquettes via a multipolar analysis of the magnetic interactions [2].

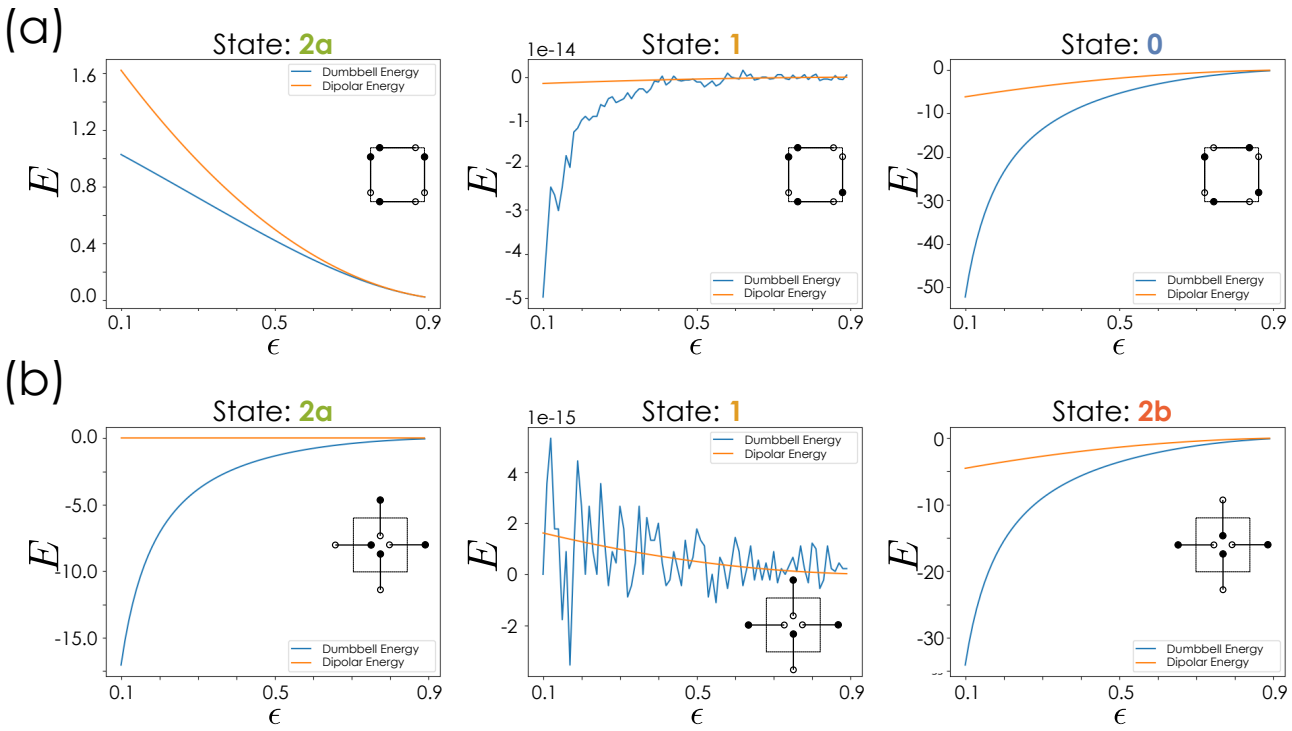

FIG. 9: Comparison between dipolar and dumbbell energies (in units of $\mu_0 q^2/(4\pi a)$) as function of ϵ for the three least energetic configurations for Loop (a) and Vertex (b) geometries. For $\epsilon \to 1$, the dumbbell and dipolar energies coincide for every configuration on these two geometries. Here we show the configurations involved in the relaxation pathway of each geometry.

Consider the displacement vector between two arbitrary charges as

$$\vec{r}_n^{\,\alpha} - \vec{r}_k^{\,\beta} = \vec{r}_{nk} + (1-\epsilon)\frac{a}{2}\left(\alpha\hat{m}_n - \beta\hat{m}_k\right) \tag{4}$$

$$= \vec{r}_{nk} + (1-\epsilon)\vec{v}_{nk}^{\,\alpha\beta}, \tag{5}$$

where $\vec{r}_{nk} = \vec{r}_n - \vec{r}_k$, $\hat{m}_i$ are the directions of the magnetic moments of the islands as defined above, α and β are the signs of the charges, and

$$\vec{v}_{nk}^{\,\alpha\beta} \equiv \frac{a}{2}\left(\alpha\hat{m}_n - \beta\hat{m}_k\right) . \tag{6}$$

Then, we can expand the inverse of the distance between these charges to second order in a parameter δ, as

$$\left|\vec{r}_n^{\,\alpha} - \vec{r}_k^{\,\beta}\right|^{-1} = \left|\vec{r}_{nk} + \vec{v}_{nk}^{\,\alpha\beta}\right|^{-1}(1+\delta)^{-1/2} \tag{7}$$

$$\approx \left|\vec{r}_{nk} + \vec{v}_{nk}^{\,\alpha\beta}\right|^{-1}\left(1 - \frac{1}{2}\delta + \frac{3}{8}\delta^2\right) , \tag{8}$$

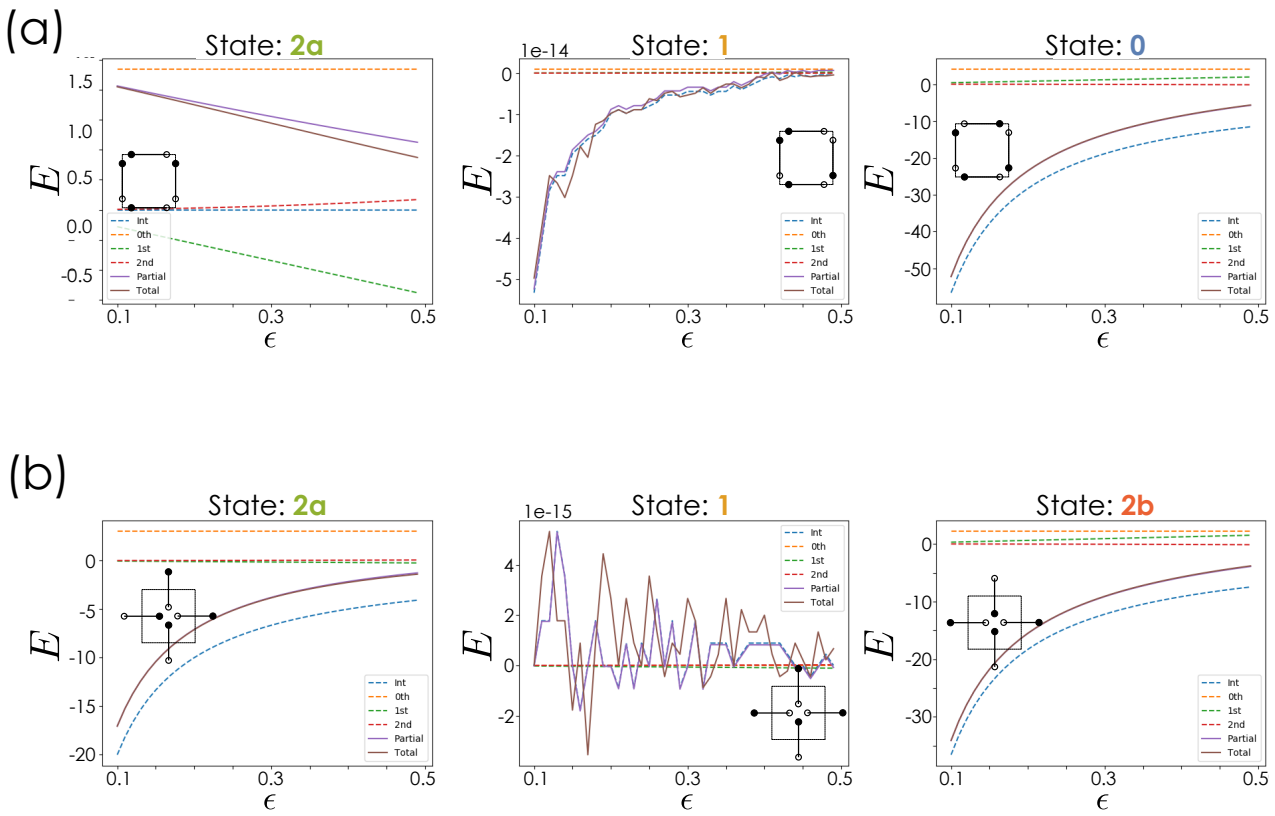

FIG. 10: Different contributions to the total dumbbell energy (in units of $\mu_0 q^2/(4\pi a)$) of the Loop (a) and Vertex (b) geometries. The dashed lines show the multipolar contributions to the energy: the internal energy (blue), the monopole/monopole contribution (yellow), the monopole/dipole contribution (green) and the second order contribution (red) that includes both dipole/dipole and quadrupole/monopole interactions. The solid lines represent the total energy of the system, computed directly from the Dumbbell definition (brown) and as a sum up to second order in ϵ in the multipolar expansion (purple).

with $\delta = \left(-2(\vec{r}_{nk} + \vec{v}_{nk}^{\alpha\beta}) \cdot \vec{v}_{nk}^{\alpha\beta}\epsilon + \left|\vec{v}_{nk}^{\alpha\beta}\right|^2 \epsilon^2\right) / \left|\vec{r}_{nk} + \vec{v}_{nk}^{\alpha\beta}\right|$.

Using this result we can finally write the total energy of the system as

$$E_c \sim \frac{\mu_0}{4\pi} \sum_{\substack{i<j \\ \alpha,\beta}} \frac{q_\alpha q_\beta}{|\vec{r}_{ij} + \vec{v}_{nk}^{\alpha\beta}|} \left[1 + \frac{(\vec{r}_{ij} + \vec{v}_{nk}^{\alpha\beta}) \cdot \vec{v}_{nk}^{\alpha\beta}}{|\vec{r}_{ij} + \vec{v}_{nk}^{\alpha\beta}|^2}\epsilon + \frac{1}{2}\left\{\frac{3((\vec{r}_{ij} + \vec{v}_{nk}^{\alpha\beta}) \cdot \vec{v}_{nk}^{\alpha\beta})^2}{|\vec{r}_{ij} + \vec{v}_{nk}^{\alpha\beta}|^3} - \frac{|\vec{v}_{nk}^{\alpha\beta}|^2}{|\vec{r}_{ij} + \vec{v}_{nk}^{\alpha\beta}|^5}\right\}\epsilon^2\right] + \mathcal{O}(\epsilon^3) \qquad (9)$$

For non-neighbour charges, $\vec{r}_{nk} + \vec{v}_{nk}^{\alpha\beta} \neq 0$ and their contribution to the total energy has terms starting from order ϵ^0. For neighbour charges in the limit $\epsilon \to 0$, their distance is $\vec{r}_{nk} + \vec{v}_{nk}^{\alpha\beta} \propto \epsilon$, and this give rise to a term of order ϵ^{-1} in the multipolar expansion. This divergent contribution to the energy is treated as an internal (self) energy E_{self} for the multipolar structures that arise when two or more charges are close together.

The multipolar moments of the magnetic structures formed by q charges have different orders in ϵ. Monopolar

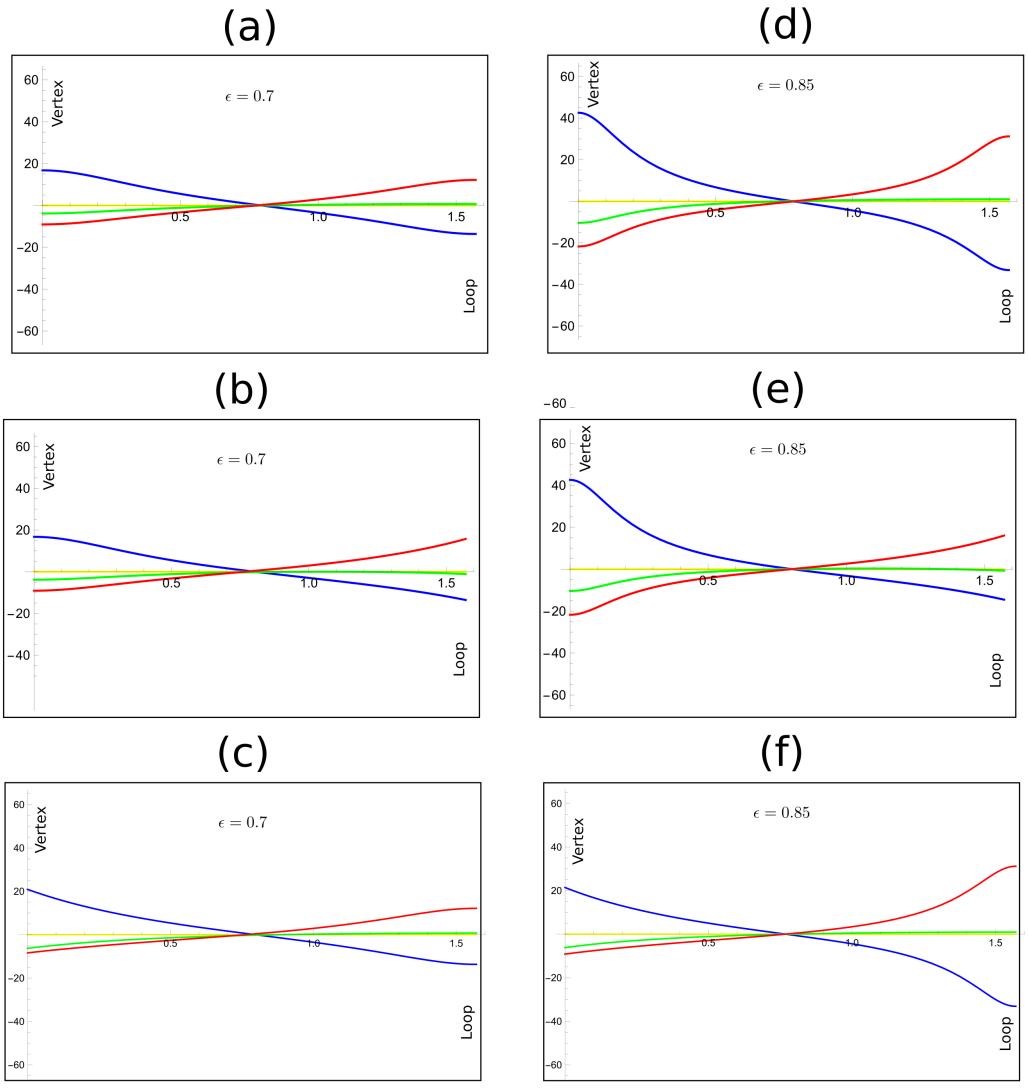

FIG. 11: Energy landscape for the rotated geometries as a function of angle ϕ for $\epsilon = 0.7$ (left) and $\epsilon = 0.85$ (right), considering dumbbell interactions. Total dumbbell energy ((a) and (d)) is well approximated by Vertex-like multipolar expansion ((b) and (e)) for $0 < \phi < \pi/4$ and by Loop-like multipolar expansion ((c) and (f)) for $\pi/4 < 0 < \pi/2$. Both multipolar expansions are truncated up to second order.

moments created by the sum of nearest neighbor q charges at a node $Q = \sum_i q_i$, contribute at order $Q \propto \epsilon^0$. Dipolar moments have a size of order ϵ and quadrupolar moments are of order ϵ^2. The couplings between the multipolar moments of magnetic structures located at different locations of a cluster can be identified in the total coulomb energy as different orders in ϵ:

$$E_{\rm c} \sim E_{\rm self} + E_{\rm mm} + E_{\rm md} + E_{\rm dd} + E_{\rm mq} + \mathcal{O}(\epsilon^3)\,, \tag{10}$$

where $E_{\rm self} \sim \epsilon^{-1}$, $E_{\rm mm} \sim \epsilon^0$, $E_{\rm md} \sim \epsilon$ and $E_{\rm dd} + E_{\rm mq} \sim \epsilon^2$, (d denotes dipole, m monopole, q quadrupole) as

illustrate din Fig.3d. We notice the different contributions to the energy can be identified by their dependence on ϵ as a power law, with exception of the term of second order, that contains the contributions both from dipole/dipole interactions and monopole/quadrupole interactions. The contributions of the different multipolar interactions to the total energy as a function of ϵ are shown in Fig.10 for the four magnetic states.

We see that for closely packed systems, the leading term of the energy is the internal energy of the magnetic structures $E_{\text{self}} \propto \epsilon^{-1}$. We will use this approach to study the behavior of the relaxation pathways for Loop and Vertex geometries.

B. Relaxation pathways for Vertex plaquettes

Vertex plaquettes ($\phi = 0$) are such that each island is oriented away from a common central node. In the dumbbell model, such central node hosts a central multipolar structure consisting of four inner q charges. Charges surrounding these are dubbed outer charges. The central node has a self energy associated with the interaction between the four charges at $\mathcal{O}(\epsilon^{-1})$. These inner charges give rise to monopoles Q that interact with the outer charges at $\mathcal{O}(0)$, and also to dipoles whose size is proportional to ϵ and which interact with outer charges at $\mathcal{O}(\epsilon)$. Dipoles of the central node can be formed at the side of the inner square and along its diagonals. Quadrupoles are also possible in the central node and they can interact with Q monopoles and contribute to the energy at $\mathcal{O}(\epsilon^2)$. Overall the multipoles of this central structure interact with the charges that surround it, and these outer charges can be treated as non-interacting among each other.

In Vertex plaquettes, the dipolar model E_{dip} yields an energy degeneracy among families $2a$ and 1 which share the same energy in this description. This degeneracy is lifted by the dumbbell model. It is easy to check that the Coulomb energy of states in the family 1 is greater than the Coulomb energy of the field-set state family $2a$. When the energy landscape of Vertex plaquettes is computed using the Coulomb interaction, an energy barrier separates state $2a$ from the ground state $2b$. In the dipolar approach this energy barrier is hidden.

The multipolar expansion for Vertex plaquettes shows that the internal energy of the central node is the dominant contribution to the energy (Fig.10b). This central node is charge neutral in state $2a$ and in the ground-state $2b$. One-flip transitions have to create and destroy central charges, therefore the intermediate state in the relaxation process (state 1) has a net charge $\pm 2q$. The dipolar magnetic moment of the node rotates and diminishes its magnitude during the transition, until such dipole moment disappears when the plaquette reaches the ground-state. The quadrupolar moment of the central structures is maximized during the relaxation, but its contribution to the total energy is negligible, compared to that of the internal energy. As the magnets are separated, the self energy competes with the Madelung energy due to the interaction between monopoles.

C. Relaxation pathways for Loop plaquettes

In Loops, magnetic islands are set in a point-to-tail configuration. The ends of adjacent islands are close, giving rise to effective Q monopoles, and dipoles arranged in a square configuration. Coulomb interactions narrow the gap between the 1 and $2a$ energies.

The multipolar expansion shows that the dominant contribution to the energy is due to the self energy in each corner of the square. The internal energy of families 1 and $2a$ is degenerate, as they relate through a permutation of the position of the multipolar structures. This degeneracy is lifted by the Madelung term due to monopolar interactions, as in state 1, the charges are closer to each other. The ground state of the system is state 0 that consists of double degenerated closed-flux configuration.

For Loop geometries the path $2a \to 1 \to 0$ has a monotonically decreasing energy. This guarantees the relaxation of the system to the groundstate, as opposed to the case of the Vertex geometries, where meta-stable configurations appear due to the monopole created when the Vertex in passing the intermediate state 1.

V. Rotated clusters

We also studied rotated structures or clusters that interpolate between the Vertex and the Loop plaquettes. To form a rotated cluster as the ones shown in Fig.6, we rotated the magnets around the z-axis an angle ϕ with respect to their own local orientation. This rotation is such that $\phi = 0$ corresponds to the Vertex geometry and $\phi = \pi/2$ corresponds to the Loop. The intermediate rotated clusters exhibit the same point symmetries of the square that the Loop and the Vertex. The $2^4 = 16$ configurations can also be grouped in 4 inequivalent families. These families are denoted following the same conventions that we have used for Vertex and Loop geometries (see Figure 6).

For $\phi \sim 0$, a group of four tips meet in the central node. For $\phi \sim \pi/2$, the tips of the magnets group at the corners of the square. In the rotated cluster with $\phi \sim \pi/4$ the tips of the magnetic islands cannot be grouped in a unique manner, as two equivalent pair of tips could be considered as closest neighbors.

Dipolar interactions divide the rotated clusters into three types: those with $0 < \phi < \pi/4$ that are close to the Vertex plaquette and share the common groundstate (namely, $2b$); those with $\pi/4 < \phi < \pi/2$ that are close to the Loop and share the common groundstate (namely, 0). The third type consists of only one cluster with $\phi = \pi/4$, with a 4-fold degenerated groundstate for all magnetic configurations. Variations in the length of the islands l or in the length of the lattice side a do not change this description, as they only produce a rescaling in the values of the energy.

Dumbbell interactions yield the same degeneracy at $\phi = \pi/4$ but only if the length of the islands l is large in comparison with a ($l/a \sim 1$). For smaller values, in particular when $l/a \leq 0.75$, the groundstate of the rotated clusters corresponds to the state $2a$, see Figure 12.

VI. Multipolar expansion for rotated clusters

Multipolar expansions are different for Loop and Vertex clusters because the geometric arrangement of the closest tips differs in both cases. As discussed above, there are rotated clusters that behave as a Loops ($0 < \phi < \pi/4$) and there are intermediate configurations that behave as a Vertex ($\pi/4 < \phi < \pi/2$). We showed that a multipolar expansion can account for the different interactions that occur at Vertex and Loop geometries.

In order to provide a multipolar expansion for rotated clusters, it is necessary to carefully define the structure of the geometry we are studying (these structures are shown in Figure 4a and Figure 7). The ϵ expansion derived in section A is of no use in this case, because there is no ϵ at which the tips of the islands meet for rotated geometries. For this reason, this time we will take the limit as the distance between closest charges goes to zero, but keeping the positions and orientations of the multipolar structures fixed. We denote our small parameter Δ and perform our multipolar expansion in terms of it, according to the illustration of Figure7. In this manner, we obtain an approximation that accounts for how the different multipolar structures contribute to the total energy for rotated geometries.

D. Multipolar expansion for rotated clusters close to the Vertex

For geometries close to the Vertex, up to second order the multipolar expansion considers five multipolar structures: one central 4-charge structure and four monopoles surrounding it. For such Vertex-like clusters we define a square of side $c = \sqrt{a^2/2 + l^2/2 + la\cos\phi}$ with its corners at the outside charges of the Vertex-like geometries (see Fig.4b and Fig.7a). Similarly there is an inner square of side $\Delta c = \sqrt{a^2/2 + l^2/2 - la\cos\phi}$, with the corner of the squares on the inner charges near the Vertex center. When ϕ changes, the squares shift their orientations by an offset angle θ, given by $\cos\theta = \frac{a^2-l^2}{\sqrt{a^4+l^4-2L^2\cos(2\phi)}}$. Considering this setting, we performed a multipolar expansion around $\Delta = 0$, with θ and c fixed. The magnetic energies for the different families of configurations are approximated by

$$\begin{aligned}
E_0 &= \frac{\mu_0 q^2}{4\pi c}\left[\frac{4+\sqrt{2}}{\Delta} + (4-11\sqrt{2}) + 4\sqrt{2}\cos(\theta)\Delta - 6\sqrt{2}\sin^2(\theta)\Delta^2 + \mathcal{O}(\Delta^3)\right], \\
E_1 &= 0, \\
E_{2a} &= \frac{\mu_0 q^2}{4\pi c}\left[-\frac{\sqrt{2}}{\Delta} + 3\sqrt{2} - 4\sqrt{2}\cos(\theta)\Delta + 2\sqrt{2}\left(2\cos^2\theta - \sin^2\theta\right)\Delta^2 + \mathcal{O}\left(\Delta^3\right)\right], \\
E_{2b} &= \frac{\mu_0 q^2}{4\pi c}\left[\frac{-4+\sqrt{2}}{\Delta} + \left(-4+5\sqrt{2}\right) + 4\sqrt{2}\cos(\theta)\Delta - 2\sqrt{2}\left(4\cos^2\theta - 5\sin^2\theta\right)\Delta^2 + \mathcal{O}(\Delta^3)\right].
\end{aligned} \tag{11}$$

up to second order in Δ. Now, the multipolar moments are in powers of Δ, with monopoles $\propto \Delta^0$, dipoles $\propto \Delta^1$ and quadrupoles $\propto \Delta^2$. The couplings between the multipolar moments of the center and the free surrounding charges can be identified in the multipolar expansion at different powers in Δ. The divergent term $E_{\text{self}} \propto \Delta^{-1}$ corresponds to the internal energy of the central node and is the dominant contribution to the energy for geometries close to $\phi = 0$.

For $\phi \sim \pi/4$ and $l/a < 0.8$, the groundstate of the system corresponds to configurations in the family $2a$, which in the multipolar expansion is explained by a reduction of the internal energy of the central structure in addition to an increase in the monopole/dipole contributions to the total energy. The Vertex-like multipolar expansion is a good quantitative approximation for the energy landscape of $0 < \phi < \pi/4$, and it also provides a good qualitative description for the energetics of the system at any given value of ϕ, as it is shown in Figure 11.

E. Multipolar expansion for rotated clusters close to the Loop

For geometries similar to the Loop $\pi/4 < \phi < \pi/2$, we define a square with corners at the midpoint between the closest nearest neighbor charges as shown in Fig.7b. The square has sides of length $b = \sqrt{a^2/4 + l^2/4 + l\sin(\phi)/2}$. The distance between the charges of a given closest neighbour pair is $b\Delta = \sqrt{a^2/2 + l^2/2 - l\sin(\phi)}$. The angle θ' between the the center of the line that joins the nearest neighboring charges, and the line that joins the center of this line and the center of the square is given by $\cos\theta' = \frac{L\cos\phi}{\sqrt{a^4/4+l^4/4+l^2\cos(2\phi)/2}}$. We expressed the Coulomb energy of the system as a function of b, θ' and Δ and expanded it around $\Delta = 0$, to obtain

$$\begin{aligned}
E_0 &= \frac{\mu_0 q^2}{4\pi b}\left[-\frac{4}{\Delta} + 4 + 2\sqrt{2}\sin(\theta')\Delta + \left[(5+\sqrt{2})\cos^2\theta' - (4+\sqrt{2}/2)\sin^2\theta'\right]\Delta^2 + \mathcal{O}(\Delta^3)\right], \\
E_1 &= 0, \\
E_{2a} &= \frac{\mu_0 q^2}{4\pi b}\left[\left(4-2\sqrt{2}\right) - 2\sqrt{2}\sin(\theta')\Delta + \left[(4+\frac{\sqrt{2}}{2})\sin^2\theta' - (\sqrt{2}+1)\cos^2\theta'\right]\Delta^2 + \mathcal{O}\left(\Delta^3\right)\right], \\
E_{2b} &= \frac{\mu_0 q^2}{4\pi b}\left[\frac{4}{\Delta} + \left(-12+4\sqrt{2}\right) + 2\sqrt{2}\sin(\theta')\Delta + \left[(\sqrt{2}-3)\cos^2\theta' - \frac{\sqrt{2}}{2}\sin^2\theta'\right]\Delta^2 + \mathcal{O}(\Delta^3)\right].
\end{aligned} \tag{12}$$

Once again the different couplings between multipolar moments can be identified as powers of Δ in the multipolar expansion for the four magnetic states. The internal energy of the 2-charge magnetic structures located near to the corners of the square is the dominant contribution to the energy for clusters close to the Loop. The groundstate for geometries close to $\phi = \pi/4$ and $\epsilon < 0.8$ is $2a$, which is explained again by an increase in the contribution of dipole/monopole interactions. The multipolar expansion truncated up to second order is a good approximation for $\pi/4 < \phi < \pi/2$ and it retrieves the behavior of the total energy for every value of ϕ and Δ, at least qualitatively.

F. Crossover at $\phi = \pi/4$

We have found that in rotated clusters multipolar interactions contributing at different orders to the total energy have a discontinuity at $\phi = \pi/4$ for the field set state $2a$ and for the ground states of Vertex and Loop $2b$ and 0 respectively. In order to examine this behavior closely we have computed the ground state energy, its first and second

derivative as a function of ϕ for clusters with ϵ_σ and ϵ_λ. The results are shown in Fig.8. In tuning with the behavior of the multipolar terms, the ground state energy shows a signature at its maximum which occurs at $\phi = \pi/4$. As a consequence, its first derivative respect to ϕ drops down almost vertically which yields what it resembles a peak in its second derivative which points to a divergence. We postpone a detailed study of the nature of this 'crossover' between Loop and Vertex like clusters for future works.

VII. Monte Carlo simulations

We performed Monte Carlo simulations of the system of nano-islands to study its relaxation to thermal equilibrium and to compare it with the results of experiments. We did not simulate the internal dynamics of each nano-island, thus there is no intrinsic blocking temperature in our simulations. As the energy of each island due to its own internal interactions is the same regardless of the direction of the magnetic moment, this does not modify the total energy of the system.

The nano-islands used in experiment have a thickness of 20nm, spins inside a single nano-island fluctuate near to the blocking temperature. In a ferromagnetic island this happens more or less when the thermal energy overcomes the exchange interaction energy of a spin with its nearest neighbors, and most likely near to the edge of the islands. The blocking temperature in experiments is expected to be approximately 780K [3]. In our model, flip a single island means that we have to flip either a single dipole or a single dumbbell that has the size of the whole naomagnet. In any case thermal energy needs to overcome the dipolar or coulomb energy between nearest neighbor dipoles or charges. This value is much larger than the blocking temperature of experiments. And therefore numerical and experimental blocking temperatures cannot be comparable in the current approach.

We performed Monte Carlo simulations considering 1000 clusters of nano-islands. We initialized every cluster in the same configuration of the family $2a$ and we let the system relax during 12000 simulation steps. At every simulation step, a random needle is selected from each cluster. If flipping the selected needle diminishes the total energy of the system, then it is flipped with probability 1. If the energy increases when the selected needle is flipped, then it is flipped with probability $e^{-\Delta E/(k_B T)}$, where ΔE is the energy difference between the flipped and the non-flipped states. The equilibrium distribution of the system corresponds to an exponential distribution of the energies, given by

$$p_n = \frac{1}{Z} e^{-\beta E_n} , \tag{13}$$

where $n = 1, \ldots, 16$ labels the different configurations and E_n is the energy of the configuration labeled n. If we consider the probability distribution associated to find the cluster in any of the four inequivalent families of

configurations, it can be written as a function of energy E as

$$p(E) = \frac{\Omega(E)}{Z} e^{-\beta E}\,, \tag{14}$$

where $\Omega(E)$ is the number of configurations in each inequivalent family. The analytical distribution of energies is shown in Fig.13.

The results of the Monte Carlo simulations show agreement with the expected equilibrium distribution, as can be seen in Fig.14. The temperature we used is high enough to overcome the energetic threshold of the vertex-like arrangement in the case of dumbbell interactions. Most simulations fully relaxed to the equilibrium state, except the Vertex plaquette with $\phi = 0$ and $\epsilon = 0.15$. This is because the temperature used is just above the temperature needed to guarantee the flipping from 2a to 1.

[1] P. Mellado, A. Concha, and L. Mahadevan, Physical review letters **109**, 257203 (2012).

[2] G. Möller and R. Moessner, Physical Review B **80**, 140409 (2009).

[3] X. Zhang, Y. Lao, J. Sklenar, N. Bingham, J. Batley, J. Watts, C. Nisoli, C. Leighton, and P. Schiffer, APL Materials **7**, 111112 (2019).

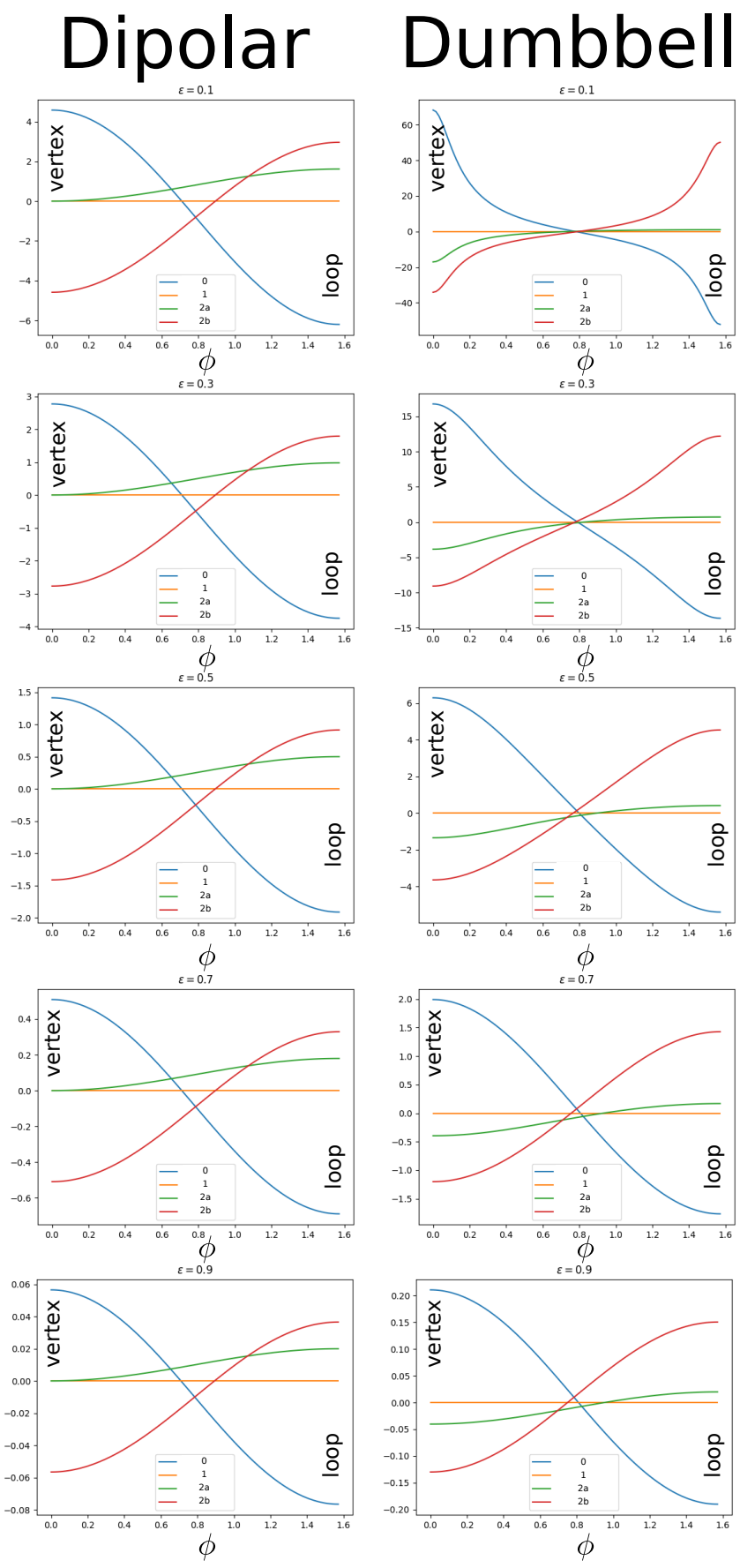

FIG. 12: Energy landscape for the four magnetic families as a function of angle ϕ and for several values of ϵ. The left panel shows the case when the energy is computed using dipolar interactions and the right panel the case of dumbbells.

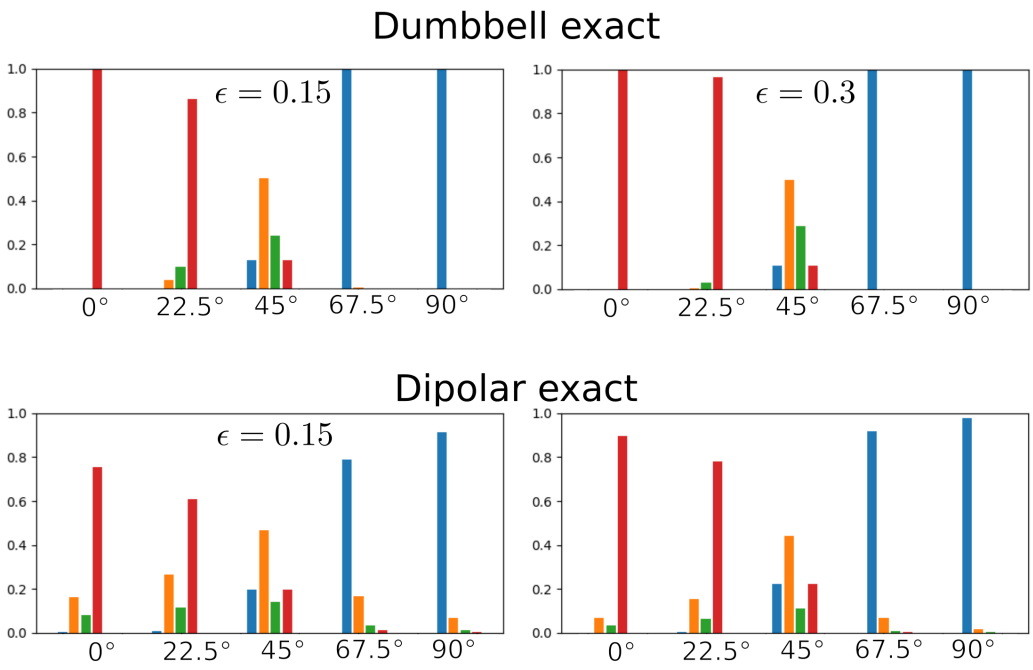

FIG. 13: Analytical equilibrium distribution for the clusters of nano-islands with different values of ϕ (labeled in the horizontal axis) and for $\epsilon = 0.15$ (left) and $\epsilon = 0.3$ (right). The blue, yellow, green and red bars indicate the probability of finding the cluster in a configuration of the families 0, 1, $2a$ and $2b$, respectively. The top panel shows the equilibrium distributions for clusters of nano-islands interacting with dumbbell interactions, while the bottom panel shows the equilibrium distributions for clusters of nano-islands interacting with dipolar interactions.

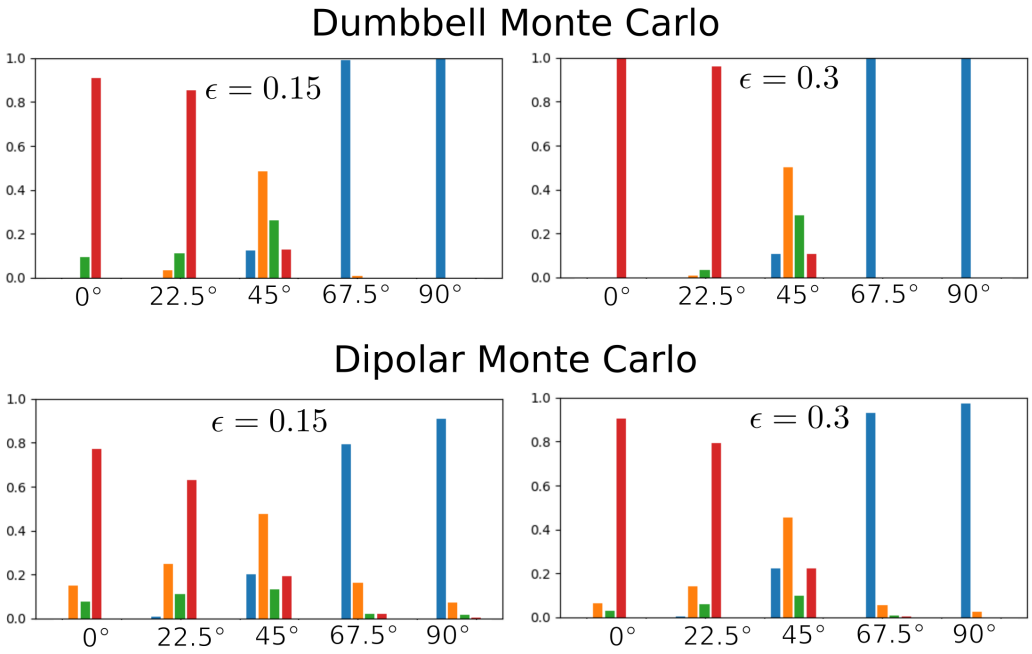

FIG. 14: Numerical distributions for the clusters of nano-islands with different values of ϕ (labeled in the horizontal axis) and for $\epsilon = 0.15$ (left) and $\epsilon = 0.3$ (right) obtained from Monte Carlo simulations. The blue, yellow, green and red bars indicate the probability of finding the cluster in a configuration of the families 0, 1, $2a$ and $2b$, respectively. The top panel shows the relaxed distributions for clusters of nano-islands interacting with dumbbell interactions, while the bottom panel shows the relaxed distributions for clusters of nano-islands interacting with dipolar interactions.